IL NUOVO CIMENTO **45 C** (2022) 60
DOI 10.1393/ncc/i2022-22060-5

COLLOQUIA: IWM-EC 2021

Status of the CLIR experiment at LNS

F. RISITANO(1)(2)(*), L. ACOSTA(3)(4), G. CARDELLA(1), E. DE FILIPPO(1), D. DELL'AQUILA(5)(6), F. FAVELA(1)(4), E. GERACI(1)(7), B. GNOFFO(1)(7), I. LOMBARDO(1), C. MAIOLINO(6), N. S. MARTORANA(6)(7), A. PAGANO(1), E. V. PAGANO(6), M. PAPA(1), S. PIRRONE(1), G. POLITI(1)(7), F. RIZZO(6)(7), P. RUSSOTTO(6), A. TRIFIRÓ(1)(2) and M. TRIMARCHI(1)(2)

(1) *INFN, Sezione di Catania - Catania, Italy*
(2) *Dipartimento di Scienze Matematiche e Informatiche, Scienze Fisiche e Scienze della Terra, Università di Messina - Messina, Italy*
(3) *INFN, Sezione di Milano - Milan, Italy*
(4) *Instituto de Física, Universidad Nacional Autónoma de México Ciudad de México, Mexico*
(5) *Dipartimento di Chimica e Farmacia, Università di Sassari - Sassari, Italy*
(6) *INFN, LNS - Catania, Italy*
(7) *Dipartimento di Fisica e Astronomia "Ettore Majorana", Università degli Studi di Catania Catania, Italy*

received 12 May 2022

Summary. — To investigate exotic cluster structures in neutron-rich nuclei via break-up reactions on a light target, the CLIR experiment was performed at INFN – Laboratori Nazionali del Sud (LNS). To this aim, a Radioactive Ion Beam (RIB) was produced, by means of the FRIBs@LNS facility, exploiting the In-Flight fragmentation technique: in this way, the obtained beam contains several radioactive ions of interest, such as ^{6}He, ^{7,8,9}Li, ^{11,12}Be, ^{13,14,15}B, ^{17}C, and even the ^{16}C and ^{10}Be isotopes, for which cluster structures have already been studied at LNS. The isotopes of the cocktail beam were identified by means of the ΔE-ToF method, and afterward break-up reactions were triggered by sending them on a $(CH_2)_n$ polyethylene (protons) target; the reaction fragments were detected by the high-granularity femtoscope array FARCOS coupled with the CHIMERA 4π multidetector. In this paper an overview of the status of the experiment will be given, and in particular the calibration procedures developed for the tagging detector and for the FARCOS array will be described.

(*) E-mail: farisitano@unime.it, fabio.risitano@ct.infn.it

1. – Introduction

The study of the cluster structure of light nuclei represents one of the most powerful tools to understand the behavior of nuclear forces in few-body interaction: as a matter of fact, it is well known that self-conjugated nuclei can present a cluster structure of α particles, as a consequence of the re-organization of nucleons in more stable sub-units [1]. These clustering effects could also be observed in non self-conjugated nuclei, in which the extra nucleons, typically neutrons, behave like valence electrons in atomic molecules, leading to high deformations and to the formation of molecular structures [2]. Some examples of interesting study cases are ^{10,11,12}Be, ^{13,14,15}B and ^{16,17}C isotopes, for which the study of cluster states is very active and growing, especially in recent years [3-5].

In particular, cluster structures play an important role in beryllium isotopes. The self-conjugated ^{8}Be isotope, as a matter of fact, is indeed unbound at ground state, while the neutron-richer isotopes ^{9,10}Be are in fact bound, since the extra one or two neutrons can provide a covalent bond between the α clusters, increasing its stability [6]. Furthermore, for the ^{10}Be case, several states have been studied, even in previous experiments performed at LNS [7], in which the rotational bands and parity suggest an $\alpha - 2n - \alpha$ molecular structure, analyzed by means of the $^{6}\mathrm{He} + {}^{4}\mathrm{He}$ decay.

Cluster structure were also predicted even in neutron-rich carbon isotopes, for example in ^{13,14}C [8], in which molecular structures have been observed. A further interesting case is represented by ^{16}C, in which exotic molecular structures was hypothesized: in this case, the four extra neutrons act in pairs of two as valence bonds for the α particles, allowing the formation of linear or triangular structures [9-11].

To investigate some of the above case studies, the CLIR experiment was performed at INFN-LNS, by using the FRIBs facility to produce a radioactive ion beam through the In-Flight fragmentation technique [12].

2. – Experimental details

A ^{18}O primary beam (55 MeV/u), accelerated by the Superconducting Cyclotron *K800* was fragmented on a 1500 μm thick ^{9}Be production target. Among the reaction products of primary beam fragmentation, some isotopic species were selected, by means of the FRIBs@LNS (in-Flight Radioactive Ions Beams at LNS) fragment separator [12], with a magnetic rigidity of $B\rho \approx 2.8$ Tm and a momentum acceptance of $\Delta p/p \approx 1.01\%$. Identification in charge and mass of the various species of the cocktail beam was performed by means of a tagging system [13], formed by a Micro Channel Plate (MCP) high-time resolution detector and a Double Sided Silicon Strip Detector (DSSSD) 156 μm thick. In this way, the ΔE-ToF technique allowed us to identify isotopes for all the species of the cocktail beam, by correlating the energy loss of each ion inside the detector and the time of flight among the two tagging detectors, ≈12.9 meters apart.

Experimental data was gathered by the FARCOS array [14], coupled with the CHIMERA 4π multidetector [15]. CHIMERA consists of 1192 two-stage Si-CsI(Tl) telescopes, covering 94% of the whole solid angle. Two different reaction targets were used, a $(CH_2)_n$ polyethylene 50 μm thick target, and a ^{12}C 75 μm thick target.

Moreover, between ring 9 and the sphere of the CHIMERA array, four three-stage FARCOS telescopes were placed at small angles around the beam, covering a polar angle of $1^\circ \leq \theta \leq 8.5^\circ$, gathering most of the reaction products. In particular, the first three rings of the CHIMERA multidetector have been turned off, as the FARCOS placement shadowed them.

Each FARCOS telescope consists of 2 DSSSD stages, 300 μm and 1500 μm thick respectively, made of a grid of 32×32 front and back strips with 2 mm pitch, covering a total area of 6.4 cm $\times$ 6.4 cm, followed by a third stage of four CsI(Tl) scintillators 6 cm thick, read out by a photodiode.

Due to its 132 different channels, each FARCOS telescope shows excellent characteristics of high granularity, high angular and energetic resolution, which makes it ideal for such experiments, in which high precision in Q-value and angular momentum calculation is needed. In the following sections, the status of the calibration of the various FARCOS stages will be described, as well as the identification of the cocktail beam species by means of a study on the ΔE-*ToF* tagging matrix.

2˙1. *Calibration of the Tagging system through the* ΔE-*ToF technique*. – The production and the energy loss of the cocktail beam was simulated by means of the LISE++ software [16], in a configuration as close as possible to the real FRIBs settings, with the aim to calibrate the tagging system.

Each one of the 32 front vertical strips of the tagging DSSSD detector has been calibrated individually, both in energy and ToF, thus obtaining the plot of fig. 1, from which identification of all the isotopic species was performed, allowing us the recognition of several different species, from ^{6}He to ^{17}C.

After calibration of the ΔE-*ToF* plot, a preliminary study on the horizontal distribution of the cocktail beam was performed, shown in fig. 2, obtained by plotting the yield of each ion in the legend for each of the 32 vertical strips. As one can easily see, ^{16}C, ^{10}Be an ^{8}Li are the most produced fragments.

2˙2. *FARCOS calibrations*. – We started by calibrating the 1500 μm thick FARCOS second detection stage: for each one of its 1024 pixels, and the corresponding CsI(Tl), we produced ΔE-E plots, as that one shown in fig. 3.

The quality of the matrix can be improved and the background noise reduced by using several different techniques. As an example, we tried to discard all the events involving the interstrip gap between two adjacent strips and by selecting a ToF window coherent with the one extracted from the ΔE-*ToF* tagging plot.

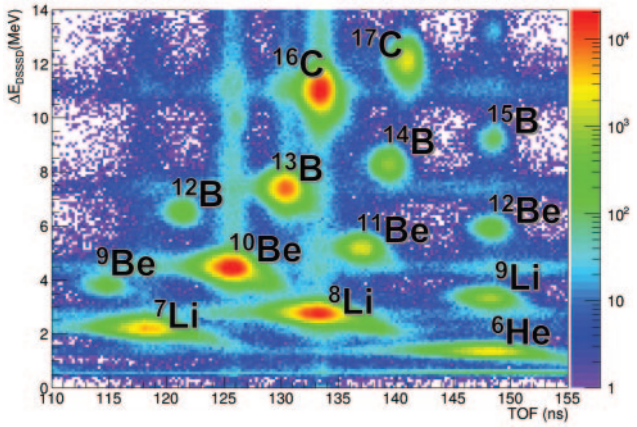

Fig. 1. – ΔE-*ToF* plot obtained from each of the 32 DSSSD strips, calibrated via simulation. All the isotopic species of the cocktail beam have been identified.

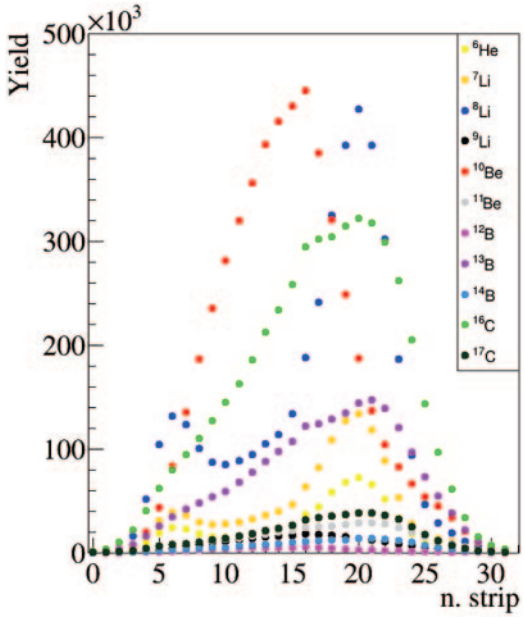

Fig. 2. – Total yield of each radioactive species of the cocktail beam, obtained for each vertical front strip of the DSSSD detector.

Cuts on the tagging ΔE-*ToF* matrix were used to recognize all the ridges belonging to each isotope of the cocktail beam. This was also necessary to identify with good precision the position of the unreacted beams on the ΔE-E matrix, passing through the reaction targets. These are characterized by distributions at the end of each isotopic ridge, and they are of crucial importance to calibrate the detector. As a matter of fact, by studying the energy loss of each unreacted beam through each stage of FARCOS, and by associating each energy to the corresponding value on the ΔE-E plot, it is possible to

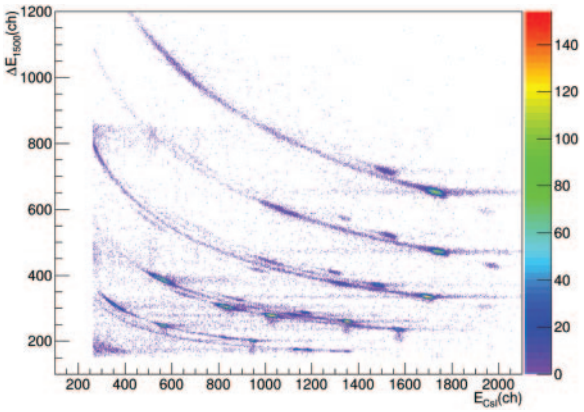

Fig. 3. – ΔE-E plot obtained from the data of a single pixel for the 1500 μm thick stage and the corresponding CsI(Tl) scintillator.

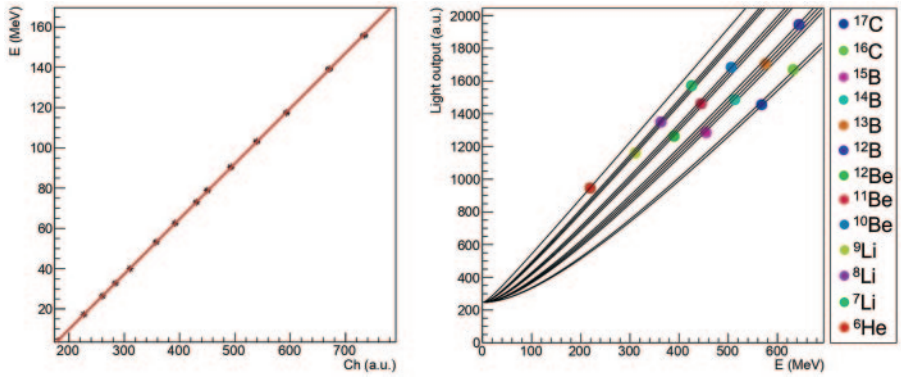

Fig. 4. – Left: linear calibration relative to a single strip of a 1500 μm thick stage of a FARCOS detector. Right: preliminary calibration obtained for a CsI(Tl) crystal of the third stage of a FARCOS detector, using the Horn formula as a fit function for each unreacted ion of the cocktail beam.

calibrate both the second and third stages. Figure 4 (left) shows an example of a linear calibration of a single strip of the 1500 μm thick stage, for which each strip has to be calibrated individually. A preliminary work on the calibration of the CsI(Tl) scintillator has been also performed, as shown in fig. 4 (right).

In this case, to take into account the non-linear behavior of the CsI(Tl) light output with energy, charge and mass of the ion impinging change, a first attempt based on the use of the Horn formula [17] was performed.

However, the missing of calibration runs and the unavailability of experimental points at lower energy made the fit more complex and further studies are needed on this matter. Calibration of several strips of the FARCOS stages allowed producing ΔE-E plots as in fig. 5, by putting together all the ΔE-E data of the calibrated strips belonging to each CsI(Tl) detector. We can appreciate a good isotopic separation for all the cocktail beam isotopes, in particular for helium and lithium isotopes, and even the separation between deuterium and tritium can be appreciated.

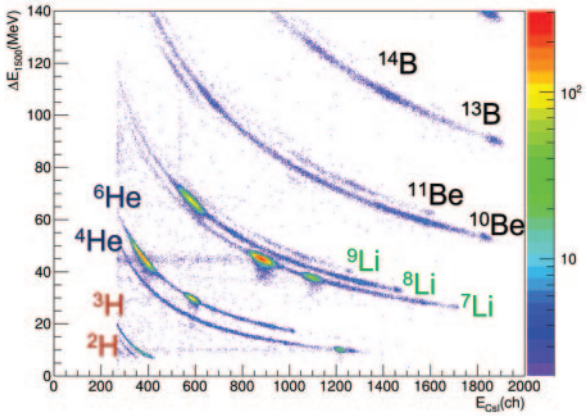

Fig. 5. – ΔE-E plot of the calibrated second stage strips and the subsequent CsI(Tl) scintillator.

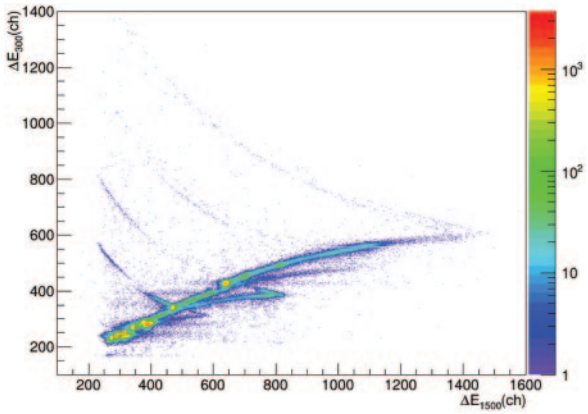

Fig. 6. – ΔE_1-ΔE_2 plot, relative to the energy loss of the ions on the first and second stage. Punching through points can be seen at the inversion of each ridge, relative for each ion.

Finally, starting from the ΔE_1-ΔE_2 matrices for the first two FARCOS stages, we performed calibration of the first 300 μm thick stage, by using the punching through spots. Since each trace is overlapped due to the presence of different isotopes of the cocktail beam (fig. 6), by performing graphical cuts on the ΔE-*ToF* tagging matrix it is possible to find the precise spot of the punching through.

3. – Preliminary work on ion selection

A preliminary analysis on the ion selection was then performed, and, due to the good performances of the FRIBs tagging system coupled with CHIMERA and FARCOS, this allowed us to observe expected break-up products.

In particular, fig. 7 shows a ΔE-E plot of the second and third stages of FARCOS, obtained by selecting the ^{10}Be isotopes, through a graphical cut in the ΔE-*ToF* tagging

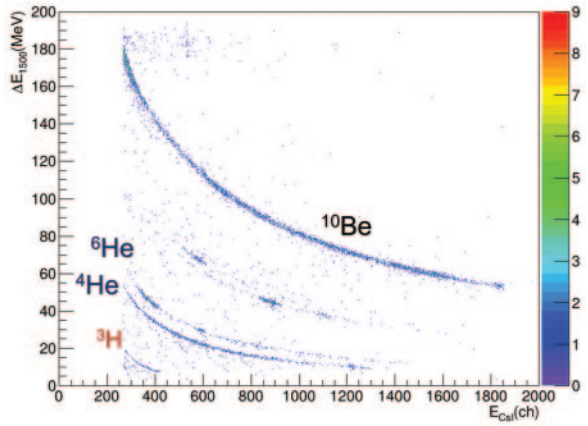

Fig. 7. – ΔE-E plot obtained by plotting the calibrated data for the second DSSSD stage, with a selection the ^{10}Be region on the tagging ΔE-*ToF* matrix.

matrix. It is possible to evidence the presence of interesting reaction products expected in emission from the break-up of ^{10}Be clustering states, namely ^{6}He + ^{4}He.

4. – Conclusions

Calibration in energy and time of flight of the 32 front strips of the DSSSD detector of the tagging system has been performed as a first step of this analysis. In particular, this calibration has been performed by means of LISE++ simulations, and it allowed us to identify all the cocktail beam isotopes produced, from ^{6}He to ^{17}C, containing in particular high yields of ^{10}Be, ^{16}C and ^{8}Li.

Furthermore, we have developed calibration strategies for the different FARCOS stages, and in particular: the 1500 μm thick second stage and the CsI(Tl) scintillator have been calibrated by using the unreacted cocktail beam energies on the ΔE-E plots, while the 300 μm thick first stage has been calibrated by using the punching through spots on ΔE_1-ΔE_2 matrices.

Furthermore, the majority of relevant strips were calibrated for all the 1500 μm thick stages of the four FARCOS telescopes, and a preliminary work on the calibration of the CsI(Tl) stages has been shown, performed with the Horn light-output formula.

As a result, a good isotopic identification of the ions of the cocktail beam was obtained, and, in particular, by using graphical cuts on the ΔE-*ToF* matrices, it was shown evidence of interesting reaction products, expected in emission from break-up reactions.

REFERENCES

[1] Ikeda K. *et al.*, *Prog. Theor. Phys. Suppl.*, **E68** (1968) 464.
[2] von Oertzen W., Freer M. and Kanada-En'yo Y., *Phys. Rep.*, **432** (2006) 43.
[3] Freer M. *et al.*, *J. Phys.: Conf. Ser.*, **381** (2012) 012009.
[4] Liu W. *et al.*, *Phys. Rev. C*, **104** (2021) 064605.
[5] Kanada-En'yo Y. *et al.*, *Phys. Rev. C*, **66** (2002) 011303.
[6] von Oertzen W., *Z. Phys. A*, **354** (1996) 37.
[7] Dell'Aquila D. *et al.*, *Phys. Rev. C*, **93** (2016) 024611.
[8] von Oertzen W. *et al.*, *Nucl. Phys. A*, **738** (2004) 264.
[9] Baba T. *et al.*, *Phys. Rev. C*, **90** (2014) 064319.
[10] Liu Y. *et al.*, *Phys. Rev. Lett.*, **124** (2020) 192501.
[11] Itagaki N. *et al.*, *Phys. Rev. C*, **64** (2001) 014301.
[12] Russotto P. *et al.*, *J. Phys.: Conf. Ser.*, **1014** (2018) 012016.
[13] Lombardo I. *et al.*, *Nucl. Phys. B*, **215** (2021) 272.
[14] Pagano E. V. *et al.*, *EPJ Web of Conferences*, **117** (2016) 10008.
[15] Pagano A. *et al.*, *Nucl. Phys. A*, **704** (2004) 504.
[16] `http://lise.nscl.msu.edu/lise.html`.
[17] Horn D. *et al.*, *Nucl. Instrum. Methods A*, **320** (1992) 273.